

## ABNORMAL SALT EFFECTS ON A CATION/ANION REACTION. AN INTERPRETATION BASED ON THE ANALYSIS OF THE COMPONENTS OF THE EXPERIMENTAL RATE CONSTANT

Francisco SANCHEZ<sup>1</sup>, Pilar PEREZ-TEJEDA<sup>2</sup>, Rafael JIMENEZ<sup>3</sup> and  
Isaac VILLA<sup>4,\*</sup>

Departamento de Química Física, Facultad de Química, Universidad de Sevilla,

c/Profesor García González s/n, 41012 Sevilla, Spain;

e-mail: <sup>1</sup> gcjrv@us.es, <sup>2</sup> pp tejeda@us.es, <sup>3</sup> rsindreu2@hotmail.com, <sup>4</sup> ivilla@us.es

Received October 27, 2008

Accepted January 23, 2009

Published online April 6, 2009

Salt effects ( $\text{NaNO}_3$ ) on the kinetics of the reactions  $[\text{Fe}(\text{CN})_6]^{3-} + [\text{Ru}(\text{NH}_3)_5(\text{pyz})]^{2+} = [\text{Fe}(\text{CN})_6]^{4-} + [\text{Ru}(\text{NH}_3)_5(\text{pyz})]^{3+}$  (pyz = pyrazine) were studied through *T*-jump measurements. An abnormal (positive) salt effect on the forward reaction was observed and a normal (negative) effect on the reverse one. These facts imply an asymmetric behavior of anion/cation reactions depending on the charge sign of the oxidant and reductant. The results can be rationalized by using the Marcus-Hush treatment for electron-transfer reactions after decomposition of the experimental rate constants into their components.

**Keywords:** Electron transfer; *T*-Jump measurements; Kinetics; Abnormal salt effect; Marcus-Hush treatment; Ferricyanide oxidation; Ruthenium complexes; Thermodynamics.

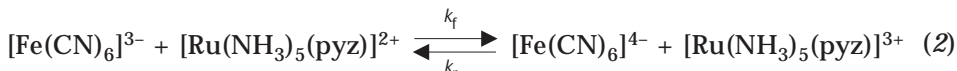
Classical theory of kinetic salt effects on anion/cation reactions, as given in current textbooks<sup>1</sup>, is based on the Brønsted equation<sup>2</sup>

$$k = k_0 \frac{\gamma_A \gamma_B}{\gamma_{\neq}}. \quad (1)$$

In this equation,  $k_0$  is the rate constant in a given reference state and  $\gamma_A$ ,  $\gamma_B$ , and  $\gamma_{\neq}$  are the activity coefficients of the reactants A, B, and the transition state  $\neq$ , corresponding to the reference state. According to the Brønsted equation, a negative salt effect is expected for anion/cation reactions and a positive salt effect is predicted for reactions of ions of the same charge sign. These predictions have been checked many times. In fact, Livingston's diagram<sup>3</sup> is a beautiful illustration of salt effects. All this is well known by chemists working in the field of chemical kinetics, up to such a point that

salt effects are taken frequently as criteria for the mechanism diagnosis. It is less known that, in the field of electron-transfer reactions, there are cases in which a positive salt effect is found for anion/cation reactions<sup>4</sup>.

To clarify these abnormal effects, a kinetic study of the reaction (2) has been carried out in  $\text{NaNO}_3$  solutions of different concentrations (1–6 mol  $\text{dm}^{-3}$ ).



The result of this study reveals the existence of abnormal salt effects for the forward reaction. However, the reverse reaction shows normal behavior. These facts can be rationalized by using the Marcus–Hush<sup>5</sup> theory of electron-transfer processes, after decomposition of the experimental rate constant into its components. In particular, we have been able to obtain the main parameters that control the kinetics of the electron-transfer reactions, the reorganization,  $\lambda$ , and reaction,  $\Delta G'$ , Gibbs energies of the processes. The knowledge of these parameters and their variations on changing the reaction medium is important. In particular, in the case of reactions between transition metal complexes, this knowledge is of interest with regard to the implications of these electron-transfer processes for the design of novel systems of technological significance (e.g., molecular electronics or sensor devices)<sup>6</sup>.

It is worth pointing out that this paper constitutes an extension of previous studies by our group<sup>7</sup> in this field. This extension regards the measurement of the equilibrium constant corresponding to the formation of the encounter complex (see hereinafter) and the introduction of the effective (dielectric) permittivity, when dealing with salt solutions. This has permitted us to obtain better values of electron-transfer rate constants.

## EXPERIMENTAL

### Materials

The complexes  $[\text{Ru}(\text{NH}_3)_5(\text{pyz})](\text{ClO}_4)_2$  (pyz = pyrazine) and  $[\text{Co}(\text{NH}_3)_5(\text{dmso})](\text{ClO}_4)_3$  (dmso = dimethylsulfoxide) were prepared and purified according to the procedure described in the literature<sup>8</sup>. The reagents  $\text{K}_4[\text{Ru}(\text{CN})_6]$ ,  $\text{Na}_3[\text{Fe}(\text{CN})_6]$  and  $\text{NaNO}_3$  of AR grade were used as purchased. The water used as the solvent had conductivity  $< 10^{-6} \text{ S m}^{-1}$ .

### Equilibrium Measurements

The equilibrium constants,  $Q$ , for reaction (2) were obtained from spectrophotometric data.

$$Q = \frac{k_f}{k_r} = \frac{[\text{Fe}(\text{CN})_6]^{4-} [\text{Ru}(\text{NH}_3)_5(\text{pyz})]^{3+}}{[\text{Fe}(\text{CN})_6]^{3-} [\text{Ru}(\text{NH}_3)_5(\text{pyz})]^{2+}} \quad (3)$$

Measurements were carried out at 472 nm, the wavelength of the maximum absorption of  $[\text{Ru}(\text{NH}_3)_5(\text{pyz})]^{2+}$  ( $\epsilon_{\text{max}} = 1.3 \times 10^4 \text{ mol}^{-1} \text{ dm}^3 \text{ cm}^{-1}$ ). A small correction for the absorption of  $[\text{Fe}(\text{CN})_6]^{3-}$  at 472 nm ( $\epsilon = 14 \text{ mol}^{-1} \text{ dm}^3 \text{ cm}^{-1}$ ) was applied. The concentrations in the mixtures of  $[\text{Fe}(\text{CN})_6]^{3-}$  and  $[\text{Ru}(\text{NH}_3)_5(\text{pyz})]^{2+}$  ranged from  $1 \times 10^{-4}$  to  $5 \times 10^{-4} \text{ mol dm}^{-3}$ . All measurements were performed at 298.2 K.

#### Determination of the Equilibrium Constant $K$ for the Formation of the Ion Pair $[\text{Co}(\text{NH}_3)_5(\text{dmso})]^{3+}/[\text{Ru}(\text{CN})_6]^{4-}$

A spectrophotometric method served for the determination of the equilibrium constant,  $K$ , for the formation of the ion pair  $[\text{Co}(\text{NH}_3)_5(\text{dmso})]^{3+}/[\text{Ru}(\text{CN})_6]^{4-}$ . Absorbance measurements were carried out with a Cary 500 Scan UV-Vis-NIR spectrophotometer. The solutions contained  $[\text{Co}(\text{NH}_3)_5(\text{dmso})]^{3+}$  and  $[\text{Ru}(\text{CN})_6]^{4-}$  at equimolar concentrations, ranging from  $1 \times 10^{-4}$  to  $6 \times 10^{-3} \text{ mol dm}^{-3}$ .

The experiments were carried out at 298.2 K, employing a 1-cm path length cell. The monitoring wavelength was 352 nm, which corresponds to the maximum of the MMCT (metal-to-metal charge transfer) band of the ion pair. The molar absorption coefficient for this ion pair was determined from the slope of the Beer's plot at concentrations corresponding to the complete formation of the ion pair (Fig. 1). Having the molar absorption coefficient, it is simple to obtain the values of  $K$  corresponding to the formation of the ion pair<sup>9</sup>.

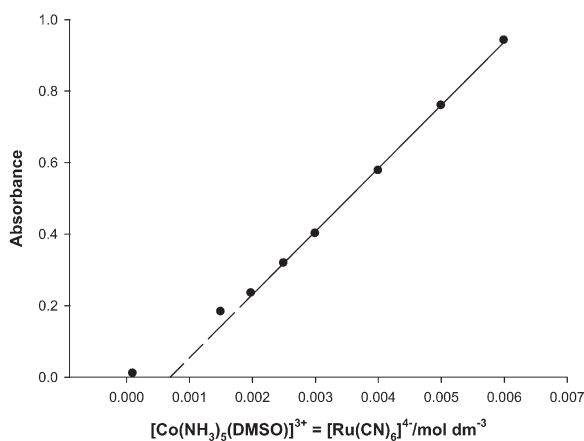


FIG. 1  
The Beer's plot of the formation of the  $[\text{Co}(\text{NH}_3)_5(\text{dmso})]^{3+}/[\text{Ru}(\text{CN})_6]^{4-}$  ion pair at 298.2 K and 0.1 M  $\text{NaNO}_3$ . Reactants at equimolar concentrations. The points are the experimental data and the line corresponds to the Beer's plot

## Kinetic Measurements

Kinetics of the reactions (2) was studied by the *T*-jump technique, using a Hi-Tech SF-61 apparatus. The concentrations of the reactants  $[\text{Ru}(\text{NH}_3)_5(\text{pyz})]^{2+}$  and  $[\text{Fe}(\text{CN})_6]^{3-}$  in the mixture ranged from  $5 \times 10^{-5}$  to  $1 \times 10^{-4}$  mol dm<sup>-3</sup>. The solutions also contained  $\text{NaNO}_3$  at desired concentrations. The initial temperature and the voltage were adjusted according to the considerations of the apparatus in such a way that the final temperature of 298.2 K was reached (after the *T*-jump). After perturbation of the system, the absorbance was recorded up to the equilibrium (at 298.2 K).

Under the experimental conditions, the relaxation time,  $\tau$ , is given by Eq. (4)

$$\frac{1}{\tau} = k_r \{ Q ( [[\text{Fe}(\text{CN})_6]^{3-}]_e + [[\text{Ru}(\text{NH}_3)_5(\text{pyz})]^{2+}]_e ) + [[\text{Fe}(\text{CN})_6]^{4-}]_e + [[\text{Ru}(\text{NH}_3)_5(\text{pyz})]^{3+}]_e \} . \quad (4)$$

In this equation,  $[\text{X}]_e$  represent the equilibrium concentrations of the species X. The values of  $Q$  are given by  $Q = k_f/k_r$ . Both rate constants,  $k_f$  and  $k_r$ , can readily be obtained from Eq. (4) and the previously measured values  $Q$ .

## RESULTS

Table I contains the values of  $Q$  and  $\tau$  corresponding to the studied salt solutions. Each value of  $Q$  and  $\tau$  was obtained in, at least, five independent experiments. The values of  $Q$  can be expressed by Eq. (5)

$$Q = Q^0 \frac{\gamma^{3-}\gamma^{2+}}{\gamma^{4-}\gamma^{3+}} \quad (5)$$

where  $\gamma$  are the activity coefficients of the ions with charges indicated, and  $Q^0 = k_f^0/k_r^0$ , i.e., the thermodynamic equilibrium constant. Taking the logarithm of  $Q$  in Eq. (5), and using the extended Debye-Hückel equation for the activity coefficients<sup>10</sup>, the result is

$$\log Q = \log Q^0 + \frac{A\sqrt{I}}{1 + \sqrt{I}} + BI . \quad (6)$$

The values of  $Q$  fit well to this equation (Fig. 2a). Thus, the values of  $Q$  in Table I are the data obtained from this fitting procedure. Analogously, the values of  $\tau$  (Fig. 2b) in Table I have been obtained by following the same procedure.

### Effective (Dielectric) Permittivity

Recently, reports on strategies to deal with solutions at high salt concentrations have appeared in the literature<sup>11</sup>. In these papers, effective ion-ion potentials are parametrized in order to include multibody effects at high ionic

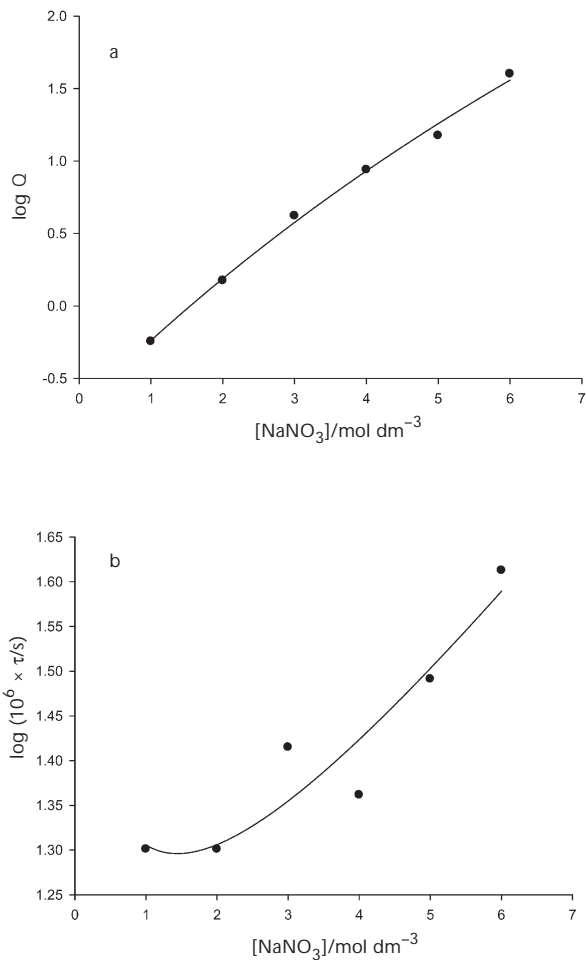


FIG. 2

a The plot of  $\log Q$  vs concentration of  $\text{NaNO}_3$ . The points are the experimental data and the line is the best fit obtained using Eq. (6). b The plot of  $\log (10^6 \tau)$  vs concentration of  $\text{NaNO}_3$ . The points are the experimental data and the line is the best fit obtained using an equation analogous to Eq. (6)

concentrations. The purpose is to capture these effects by employing a concentration dependent (relative) permittivity. Using the same idea we have obtained concentration-dependent (relative) permittivity from the experimental values of the formation constant of the ion pair  $[\text{Co}(\text{NH}_3)_5(\text{dmso})]^{3+}/[\text{Ru}(\text{CN})_6]^{4-}$ .

Figure 3 gives the formation constant  $K$  of the  $[\text{Co}(\text{NH}_3)_5(\text{dmso})]^{3+}/[\text{Ru}(\text{CN})_6]^{4-}$  ion pair, at different salt concentrations. Some data in Fig. 3

TABLE I

Equilibrium constant,  $Q$ , and relaxation time,  $\tau$ , for the reaction  $[\text{Fe}(\text{CN})_6]^{3-} + [\text{Ru}(\text{NH}_3)_5(\text{pyz})]^{2+} \xrightleftharpoons[k_r]{k_f} [\text{Fe}(\text{CN})_6]^{4-} + [\text{Ru}(\text{NH}_3)_5(\text{pyz})]^{3+}$

$[\text{NaNO}_3]$ , mol dm $^{-3}$	$Q$	$10^6 \tau$ , s
1.0	0.6	20
2.0	1.6	20
3.0	3.8	23
4.0	8.0	26
5.0	18	32
6.0	37	39

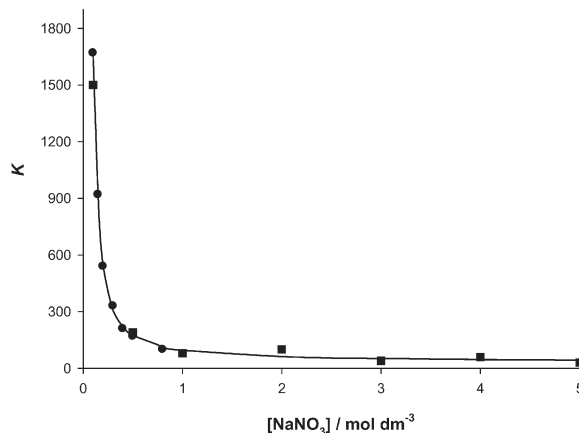


FIG. 3

Values of  $K$  (equilibrium constant corresponding to the formation of  $[\text{Co}(\text{NH}_3)_5(\text{dmso})]^{3+}/[\text{Ru}(\text{CN})_6]^{4-}$  ion pair) obtained from spectroscopic (●) and kinetic (■) measurements at several  $\text{NaNO}_3$  concentrations

correspond to the values of  $K$  for  $[\text{Co}(\text{NH}_3)_5(\text{H}_2\text{O})]^{3+}/[\text{Fe}(\text{CN})_6]^{4-}$  ion pair<sup>12</sup>. These data were obtained following a kinetic procedure different from the one employed here. However, as can be seen from Fig. 3, there is a good match between the two data sets.

In order to show that the values of  $K$ , calculated from the effective (different) values of the (relative) permittivity, are independent of the model used in the calculations, we will consider two different approaches: the Eigen–Fuoss (EF)<sup>13</sup> and the exponential mean spherical approximation (emsa)<sup>14</sup>. According to these formulations,  $K$  is given by Eq. (7)

$$k = \frac{4 \times 10^3 \pi N_A a^3}{3} \exp\left(-\frac{V_{\text{AD}}^i(a, I)}{k_B T}\right) \quad (7)$$

where  $V_{\text{AD}}^i(a, I)$  represents the mean force potential between the ions (A and D) forming the ion pair, at distance  $a$  and ionic strength  $I$ .

$$V_{\text{AD}}^{\text{EF}} = \frac{Z_A Z_D e^2}{4 \pi \epsilon_0 \epsilon_s a (1 + \kappa a)} \quad (8)$$

$$V_{\text{AD}}^{\text{emsa}} = \frac{Z_A Z_D e^2}{4 \pi \epsilon_0 \epsilon_s a (1 + \Gamma \sigma_A) (1 + \Gamma \sigma_D)} \quad (9)$$

In Eqs (7)–(9),  $N_A$  represents the Avogadro number,  $Z_A$  and  $Z_D$  are the valences of the ions,  $e$  is the proton charge,  $\epsilon_0$  the vacuum permittivity,  $a$  the contact distance of the ions in the ion pair (taken as the sum of ionic radii),  $\epsilon_s$  the (relative) permittivity of the solvent,  $\kappa$  the Debye screening parameter,  $\Gamma$  the mean spherical approximation (msa) screening parameter (the screening parameters are proportional to  $I$ ), and  $\sigma_A$  and  $\sigma_D$  are the diameters of the ions. These radii (or diameters) have been calculated using Eq. (10)<sup>15</sup>

$$r = \frac{1}{2} (l_1 l_2 l_3)^{1/3} \quad (10)$$

where  $l_i$  are the lengths of the three different L–M–L' axes in the complexes<sup>16</sup>. The  $r$  values are given in Table II.

It is clear that from the data in Fig. 3 and Eqs (7)–(10) it is possible to get the effective solvent (relative) permittivity,  $\epsilon_s^{\text{eff}}$ , corresponding to EF and

emsma approaches, once the radii have been calculated. The values of  $\epsilon_s^{\text{eff}}$  for these approaches are given in Table III.

One can see that the effective values of the (relative) permittivity to be used in the application of the EF or emsa treatments are of the same order of magnitude as experimental values<sup>17</sup>, but somewhat lower. This behavior of the (relative) permittivity is similar to the findings of other studies that employ concentration-dependent (relative) permittivity, calculated by simulation methods<sup>11,18</sup>. It is worth pointing out that in these papers, like

TABLE II  
Radii of the complexes studied

Complex	$r, \text{\AA}$
$[\text{Fe}(\text{CN})_6]^{3-}$	4.6
$[\text{Ru}(\text{NH}_3)_5(\text{pyz})]^{2+}$	4.3
$[\text{Ru}(\text{CN})_6]^{4-}$	4.7
$[\text{Co}(\text{NH})_3)_5(\text{dmso})]^{3-}$	3.8

TABLE III  
Dielectric permittivities,  $\epsilon_s$  (experimental and effective values) at 298.2 K

$[\text{NaNO}_3]$ , mol dm <sup>-3</sup>	$\epsilon_{\text{exp}}^a$	$\epsilon_{\text{EF}}$	$\epsilon_{\text{emsma}}$
0.1	76.9	55.7	53.3
0.15	76.1	54.1	51.0
0.2	75.4	53.0	49.3
0.3	74.0	51.2	46.7
0.4	72.7	49.5	44.1
0.5	71.5	48.0	42.0
0.8	68.0	43.5	36.5
1.0	65.8	40.8	33.5
2.0	56.8	30.7	23.2
3.0	50.1	24.3	17.4
4.0	45.2	20.4	13.8
5.0	42.0	17.6	11.7

<sup>a</sup> From ref.<sup>17</sup>

here, the effective (relative) permittivity is dependent on the model type (of the potentials) employed in the simulations.

We employed the effective values of the solvent (relative) permittivity to calculate the formation constants of the encounter complex of the electron-transfer reactions, from separate donor and acceptor. These values are necessary in order to separate the true electron-transfer rate constant from  $k_f$  and  $k_r$ , the experimental rate constants (see below).

## DISCUSSION

From the data in Table I, the values of  $k_r$  and  $k_f$  have been obtained. These values are given in Table IV. As mentioned hereinbefore, these rate constants show opposite trends when the salt concentration is varied. The trend of  $k_r$  can be considered normal, according to the classical theory of salt effects. On the contrary, the trend of  $k_f$  can be considered abnormal according to this theory.

Under the conditions prevailing in this work,  $K[R] \ll 1$ , where  $K$  is the equilibrium constant corresponding to the formation of the encounter complex and  $[R]$  the concentration of the reactant (donor or acceptor) in excess, the values of  $k_f$  and  $k_r$  are given by Eqs (11a) and (11b), respectively

$$k_f = K_f k_{et}^f \quad (11a)$$

and

$$k_r = K_r k_{et}^r. \quad (11b)$$

TABLE IV

Rate constants for the forward and reverse reactions  $[\text{Fe}(\text{CN})_6]^{3-} + [\text{Ru}(\text{NH}_3)_5(\text{pyz})]^{2+} \rightleftharpoons [\text{Fe}(\text{CN})_6]^{4-} + [\text{Ru}(\text{NH}_3)_5(\text{pyz})]^{3+}$

$[\text{NaNO}_3]$ , mol dm $^{-3}$	$10^{-8} k_f$ mol $^{-1}$ dm $^{-3}$ s $^{-1}$	$10^{-8} k_r$ , mol $^{-1}$ dm $^{-3}$ s $^{-1}$
1.0	4.8	7.5
2.0	5.2	3.6
3.0	5.8	1.8
4.0	6.3	0.8
5.0	6.9	0.4
6.0	7.6	0.2

The values of  $K_f$  and  $K_r$  were determined using EF and emsa approaches, and the effective (relative) permittivity. The values of  $K_f$  and  $K_r$ , as well those of  $k_{et}^f$  and  $k_{et}^r$  are presented in Table V. A good agreement is found for the values obtained following the two approaches.

Now, the reason for the normal behavior of  $k_r$  and the abnormal behavior of  $k_f$  are apparent: in the case of  $k_r$ , its components  $K_r$  and  $k_{et}^r$  decrease as the salt concentration is increased. In the case of  $k_f$ ,  $K_f$  decreases, but  $k_{et}^f$  increases as the salt concentration is increased. Thus, the abnormal behavior of  $k_f$  is due to the fact that the true electron-transfer process, i.e., the electron transfer within the encounter complex



shows a positive salt effect, which is more marked, and thus the negative salt effect on  $K_f$ . On the contrary, in the case of the components of  $k_r$ , both  $k_{et}^r$  and  $K_r$  show a negative salt effect.

To deeper insight into the different behavior of  $k_{et}^f$  and  $k_{et}^r$  with regard to salt effects, the Marcus-Hush theory for the electron-transfer processes was used. According to this treatment, the rate constant for processes of this kind is given<sup>19</sup> by Eq. (13)

$$k_{et} = \kappa_{el} \nu_n e^{-\Delta G^\ddagger / RT}. \quad (13)$$

TABLE V  
Equilibrium constants of precursor complex formation,  $K$  (mol<sup>-1</sup> dm<sup>-3</sup>), and electron-transfer rate constants,  $k_{et}$  (s<sup>-1</sup>), following EF and emsa approaches for forward, f, and reverse, r, reactions at 298.2 K

[NaNO <sub>3</sub> ] <sup>a</sup>	$K_f^{\text{EF}}$	$K_f^{\text{emsu}}$	$K_r^{\text{EF}}$	$K_r^{\text{emsu}}$	$k_{et,f}^{\text{EF}} \text{ } b$	$k_{et,f}^{\text{emsu}} \text{ } b$	$k_{et,r}^{\text{EF}} \text{ } c$	$k_{et,r}^{\text{emsu}} \text{ } c$
1.0	11.1	10.7	69.1	64.2	4.3	4.5	10.9	11.7
2.0	8.9	8.6	45.0	41.1	5.9	6.1	8.0	8.8
3.0	8.3	7.9	38.5	34.8	7.0	7.3	4.5	5.0
4.0	7.8	7.5	34.6	31.9	8.1	8.4	2.4	2.6
5.0	7.6	7.2	32.2	29.1	9.1	9.6	1.3	1.4
6.0	6.9	6.4	26.9	22.9	11.0	11.9	0.7	0.8

<sup>a</sup> Concentration in mol dm<sup>-3</sup>; <sup>b</sup>  $k_{et,f} \times 10^{-7}$ ; <sup>c</sup>  $k_{et,r} \times 10^{-6}$ .

Here  $\kappa_{\text{el}}$ ,  $\nu_{\text{n}}$  and  $\Delta G^\ddagger$  are the electronic transmission coefficient, nuclear frequency factor, and Gibbs energy of activation, respectively. The latter is given by Eq. (14)

$$\Delta G^\ddagger = \frac{(\lambda + \Delta G')^2}{4\lambda} . \quad (14)$$

The parameter  $\lambda$  in Eq. (14) is the so-called Gibbs energy of reorganization for the electron-transfer process (Eq. (12)). This Gibbs energy consists of a solvent contribution,  $\lambda_s$ , an ionic atmosphere contribution,  $\lambda_{\text{at}}$ , and a contribution arising from the internal reorganization of the donor and the acceptor,  $\lambda_{\text{in}}$ . The latter is usually considered to be independent of the reaction media.

Except for strongly nonadiabatic processes, the pre-exponential term in  $k_{\text{et}}$  is of the order of the (average) vibrational frequency promoting the activation of the precursor complex. Thus, a value of  $10^{12}$ – $10^{13}$  s<sup>−1</sup> seems reasonable. In the following calculations, a value of  $6.2 \times 10^{12}$  s<sup>−1</sup> was used. This value corresponds to that of the pre-exponential factor in the expression of the rate constant given by the classical transition state theory ( $k_{\text{B}}T/h$ ) at our experimental temperature. In this way,  $\Delta G^\ddagger$  can be obtained from  $k_{\text{et}}$  (Eq. (15))

$$\Delta G^\ddagger = -RT \ln \frac{k_{\text{et}}}{6.2 \times 10^{12}} . \quad (15)$$

The parameter  $\Delta G'$  in Eq. (14) is the (standard formal) Gibbs energy corresponding to the electron-transfer process (Eq. (12)), which produces the successor complex from the precursor complex. This parameter is different from  $\Delta G$ , the (standard formal) Gibbs energy of the reaction, which produces the separate products from the separate reactants (Eq. (2)). The latter is, of course,

$$\Delta G = -RT \ln Q \quad (16)$$

and can be calculated from the values of  $Q$  in Table I. The  $\Delta G$  and  $\Delta G'$  values are related, through,

$$\Delta G' = \Delta G + \omega_{\text{P}} - \omega_{\text{R}} . \quad (17)$$

Here  $\omega_{\text{R}}$  and  $\omega_{\text{P}}$  are the Gibbs energies corresponding to the formation of the precursor complex from the separate reactants and the formation of the successor complex from the separate products.

For the forward reaction

$$\omega_R = -RT \ln K_f \quad (18)$$

and

$$\omega_P = -RT \ln K_r. \quad (19)$$

In this way, from Eqs (16)–(19), the values of  $\Delta G'_f$  in Table VI can be calculated (clearly  $\Delta G'_r = -\Delta G'_f$ ).

Finally, the values of  $\lambda_f$  and  $\lambda_r$  have been calculated from  $\Delta G'_f$  and  $\Delta G'_r$  using Eq. (14). These values are presented in Table VI. We have found that  $\lambda_f$  and  $\lambda_r$  are the same, in agreement with the Marcus–Hush theory.

Apparently, the different salt effects on  $k_{et}^f$  and  $k_{et}^r$  are due to the differences in  $\Delta G'$ . That is, the forward reaction becomes more favorable when the salt concentration increases and (obviously) the opposite is true for the reverse reaction. These facts are the consequences of the character (anion or cation) of the donor and acceptor in these reactions. Thus, in the case of the forward reaction, the donor is a cation and the acceptor an anion. For this reaction, the donor  $[\text{Fe}(\text{CN})_6]^{3-}$ , becomes a more powerful oxidant and  $[\text{Ru}(\text{NH}_3)_5(\text{pyz})]^{2+}$  a more reductant species in the presence of the salts. This is clearly seen from Eq. (20) which gives the standard formal redox potential of a given ox/red couple

$$E^{0'} = E^0 + \frac{RT}{F} \ln \frac{\gamma_{\text{ox}}}{\gamma_{\text{red}}}. \quad (20)$$

TABLE VI

Gibbs energy change,  $\Delta G'_r = -\Delta G'_f$ , and reorganization energy,  $\lambda$ , following EF and emsa approaches for forward, f, and reverse, r, reactions of electron transfer at 298.2 K<sup>a</sup>

$[\text{NaNO}_3]$ , mol dm <sup>-3</sup>	$\Delta G'_{f,\text{EF}}$	$\Delta G'_{f,\text{emsa}}$	$\lambda_{\text{EF}}$	$\lambda_{\text{emsa}}$
1.0	-3.1	-3.0	122.7	122.2
2.0	-5.2	-5.1	124.3	123.7
3.0	-7.1	-7.0	125.9	125.3
4.0	-9.0	-8.9	127.6	126.8
5.0	-10.7	-10.6	129.2	128.4
6.0	-12.3	-12.1	130.9	129.9

<sup>a</sup> All energies in kJ mol<sup>-1</sup>.

For the  $[\text{Fe}(\text{CN})_6]^{3-/-4}$  pair, both  $\gamma_{\text{ox}}$  and  $\gamma_{\text{red}}$  decrease with increasing the salt concentration. However, the decrease in  $\gamma_{\text{red}}$  is more marked because of the higher absolute charge of the reduced form of this pair. Thus,  $E^0'$  increases as the salt concentration increases. On the contrary, for the cationic pair ( $[\text{Ru}(\text{NH}_3)_5(\text{pyz})]^{3+/2+}$  herein), the effect of the salt is to decrease  $E^0'$ , because  $\gamma_{\text{ox}}$  decreases more than  $\gamma_{\text{red}}$ . Consequently, the forward reaction becomes more favorable from a thermodynamic point of view, and this produces the abnormal salt effect. For the reverse reaction, similar arguments help to explain that  $k_r$  decreases as the salt concentration increases.

A conclusion emerges from the previous discussion. In the anion/cation electron-transfer reactions, salt effects operate in opposite directions on  $K$  and  $k_{\text{et}}$ , when the oxidant is an anion. This is because  $K$  decreases as the salt concentration increases, and  $k_{\text{et}}$  increases because the true electron-transfer reaction becomes more favorable from a thermodynamic point of view. Therefore, the sign of the salt effect on an observed rate constant ( $k = K k_{\text{et}}$ ) depends on the magnitude of these effects. If the increase in  $k_{\text{et}}$  is higher than the decrease in  $K$ , when the salt concentration increases, then a positive salt effect is observed (as reported herein). However, if the decrease in  $K$  is higher than the increase in  $k_{\text{et}}$ , then a negative salt effect will be observed.

For anion/cation electron-transfer reactions in which the oxidant is the cation, salt effects on  $k_{\text{et}}$  and  $K$  go in the same direction. Consequently, in this case, a negative salt effect is always observed.

## SYMBOLS

$a$	contact distance of the ions
$E^0$	standard redox potential
$E^0'$	standard formal redox potential
$I$	ionic strength
$k_{\text{et}}$	electron-transfer rate constant
$k_f$	forward rate constant
$k_r$	reverse rate constant
$K$	equilibrium constant for ion-pair formation
$l_i$	length of the ligand-metal-ligand axes
$Q$	apparent equilibrium constant
$Q^0$	thermodynamic equilibrium constant
$V_{\text{AD}}^1$	ionic mean force potential
$\Delta G^{\circ}$	Gibbs energy of activation
$\gamma$	activity coefficient
$\Gamma$	msa screening parameter
$\epsilon$	molar absorption coefficient
$\epsilon_s$	solvent (relative) permittivity

$\epsilon_s^{\text{eff}}$	effective solvent (relative) permittivity
$\epsilon_0$	vacuum permittivity
$\kappa$	Debye screening parameter
$\kappa_{\text{el}}$	electronic transmission coefficient
$\lambda$	reorganization energy
$v_n$	nuclear frequency factor
$\sigma$	diameter of an ion
$\tau$	relaxation time
$\omega_p$	Gibbs energy for the formation of successor complex from the separate products
$\omega_r$	Gibbs energy for the formation of precursor complex from the separate reactants

*This work was financed by the Dirección General de Investigación Científica y Técnica (DGICYT) (CTQ 2005-01392/BQU) and the Consejería de Educación y Ciencia de la Junta de Andalucía. I. Villa thanks the Ministerio de Educación y Ciencia (MEC) for their financial support through AP-2003-1155.*

## REFERENCES AND NOTES

1. Laidler K. J.: *Chemical Kinetics*, 2nd ed., p. 202. McGraw-Hill, London 1965.
2. Brönsted J. N. Z.: *Phys Chem.* **1922**, *102*, 169.
3. Livingston R. J.: *Chem. Educ.* **1930**, *7*, 2887.
4. a) Burgess J., Sánchez F., Morillo E., Gil A., Tejera J. I., Galán E., García J. M.: *Transition Met. Chem.* **1986**, *11*, 166; b) Muñoz E., Graciani M. M., Jiménez R., Rodríguez A., Moyá M. L., Sánchez F.: *Int. J. Chem. Kinet.* **1994**, *26*, 299.
5. a) Marcus R. A.: *Annu. Rev. Phys. Chem.* **1964**, *15*, 155 and references therein; b) Hush N. S.: *J. Chem. Phys.* **1958**, *28*, 962.
6. Newton M. D.: *Coord. Chem. Rev.* **2003**, *238*–*239*, 167.
7. a) Sanchez F., Perez-Tejeda P., Lopez-Lopez M.: *Inorg. Chem.* **1999**, *38*, 1780; b) Morillo M., Denk C., Perez P., Lopez M., Sanchez A., Prado P., Sanchez F.: *Coord. Chem. Rev.* **2000**, *204*, 173; c) Lopes-Costa T., Lopez-Cornejo P., Villa I., Perez-Tejeda P., Prado-Gotor P., Sanchez F.: *J. Chem. Phys. A.* **2006**, *110*, 4196.
8. a) Creutz C., Taube H.: *J. Am. Chem. Soc.* **1973**, *95*, 1086; b) Dixon N. E., Jackson W. G., Lancaster M. J., Lawrence G. A., Sargeson A. M.: *Inorg. Chem.* **1981**, *20*, 470.
9. Curtis J. C., Meyer T. J.: *Inorg. Chem.* **1982**, *21*, 1562.
10. Koryta J., Dvořák J., Boháčková V.: *Electrochemistry*, p 32. Methuen, London 1980.
11. a) Hess B., Holm C., van der Vegt N.: *Phys. Rev. Lett.* **2006**, *96*, 147801; b) Hess B., Holm C., van der Vegt N.: *J. Chem. Phys.* **2006**, *124*, 164509; c) Hess B., Holm C., van der Vegt N.: *J. Chem. Phys.* **2007**, *127*, 234508.
12. Galan M., Jimenez R., Sanchez F.: *Ber. Bunsen-Ges. Phys. Chem.* **1993**, *97*, 16.
13. a) Eigen M.: *Z. Phys. Chem. (Frankfurt am Main)* **1954**, *1*, 176; b) Fuoss R. M.: *J. Am. Chem. Soc.* **1958**, *80*, 5059.
14. a) Andersen H. C., Chandler D.: *J. Phys. Chem.* **1977**, *81*, 1311; b) Simonin J. P., Hendrawan H.: *Phys. Chem. Chem. Phys.* **2001**, *3*.
15. Brunschwig B. S., Ehrenson S., Sutin N.: *J. Phys. Chem.* **1986**, *90*, 3657.

16. To calculate  $l_i$ , van der Waals radii of the ligands have been used and metal-ligand distances have been obtained from Cambridge Structural Database (<http://www.ccdc.cam.ac.uk/>) and Inorganic Crystal Structural Database (ICSD) (<http://icsdweb.fiz-karlsruhe.de/>).
17. Barthel J., Buchner R., Münsterer N.: *Electrolyte Data Collection*, Part 2. DECHEMA, Frankfurt am Main 1975.
18. As examples: a) Fawcett R. W., Tikanen A. C. T.: *J. Chem. Phys.* **1996**, *100*, 4251;  
b) Fawcett R. W., Tikanen A. C. T.: *J. Electroanal. Chem.* **1977**, *439*, 107.
19. Marcus R. A., Sutin N.: *Biochim. Biophys. Acta* **1985**, *811*, 265.